Supporting Information

Monitoring Dynamic Cellular Redox Homeostasis Using Fluorescence-Switchable Graphene Quantum Dots

Nan Li,[1] Aung Than,[1] Chencheng Sun,[2] Jingqi Tian,[1] Jie Chen,[1] Kanyi Pu,[1] Xiaochen Dong,[2] Peng Chen*[1]*

[1] Division of Bioengineering, School of Chemical & Biomedical Engineering, Nanyang Technological University, 70 Nanyang Drive, Singapore 637457

E-mail: chenpeng@ntu.edu.sg

[2] Key Laboratory of Flexible Electronics (KLOFE) & Institute of Advanced Materials (IAM), Jiangsu National Synergetic Innovation Center for Advanced Materials (SICAM), Nanjing Tech University (NanjingTech), 30 South Puzhu Road, Nanjing 211816, China

E-mail: iamxcdong@njtech.edu.cn

Abbreviation list:

GQD, graphene quantum dots; DFOB, desferrioxamine B; H_2O_2, hydrogen peroxide; AA, ascorbic acid; NADH, nicotinamide adenine dinucleotide hydrogen; GSH, glutathione; PMA, phorbol myristate acetate; ROS, reactive oxygen species; HMSC, Human Mesenchymal Stem Cells; PL, photoluminescence; LOD, limit of detection; PET, photo-induced electron transfer; TEM, transmission electron microscopy; AFM, atomic force microscopy; DLS, dynamic light scattering; FTIR, Fourier transform infrared spectroscopy; PAGE, polyacrylamide gel electrophoresis; XPS, X-ray photoelectron spectroscopy.

Table S1 Ascorbic acid detection: our method *vs.* others.

Method	Material	Linear range (M)	Limit of Detection(M)	Reference
Colorimetry	Au nanorods@silica	1×10^{-7} to 2.5×10^{-6}	4.9×10^{-8}	Nanoscale, 2011, 3, 1756–1759
Colorimetry	Ag nanoparticles	0 to 3.5×10^{-3}	1×10^{-5}	Tanlanta, 2015, 141, 188–194
Colorimetry	CuNPs@carbon matrix	1×10^{-5} to 1×10^{-3}	1.4×10^{-6}	Chem. Eur. J. 2014, 20, 16377–16383
Colorimetry	Au nanoparticles	2×10^{-7} to 1×10^{-5}	1.7×10^{-7}	Talanta, 2013, 104, 22–26
Colorimetry	Ag nanoclusters	2×10^{-6} to 5×10^{-5}	1.6×10^{-5}	Spectrochim. Acta. A, 2013, 106, 224-30
Electrochemistry	Au-Pd/reduced graphene oxide	3×10^{-8} to 1×10^{-5}	1.5×10^{-8}	Mater. Sci. Eng. C, 2016, 68, 805–813
Electrochemistry	MWCNTs/$ZnCrFeO_4$	4×10^{-7} to 7×10^{-4}	3×10^{-8}	Mater. Sci. Eng. C, 2016, 69, 1–11
Electrochemistry	poly(phenylenediamine-aminophenol)	1×10^{-4} to 1×10^{-2}	3.6×10^{-5}	Anal. Chim. Acta, 2014, 809, 54–60
Electrochemistry	Pt nanowires/glass carbon electrode	2.5×10^{-5} to 9×10^{-4}	2×10^{-7}	Biosens.Bioelectron., 2010, 26,1056–1061
Fluorescence	Au NPs/fluorescein/ DNA	2.5×10^{-6} to2×10^{-5}	2.5×10^{-6}	Biosens.Bioelectron., 2012, 33, 241–246
Fluorescence	7-hydroxycoumarin/ MnO2 nanosheets	5×10^{-7} to 4×10^{-5}	9×10^{-8}	Anal. Chem. 2014, 86, 12206−12213
Fluorescence	Ag NPs	4×10^{-6} to 1×10^{-4}	1×10^{-7}	Luminescence, 2009, 24, 367−71
Fluorescence	nitrogen-doped -GQDs	1×10^{-6} to 9×10^{-5}	1.8×10^{-8}	J Fluoresc., 2016, 26, 1755-62
Fluorescence	nitrogen-doped carbon nanoparticles	2×10^{-7} to 1.5×10^{-4}	5×10^{-8}	Anal. Chem. 2015, 87, 8524−8530
Fluorescence	GQDs	3×10^{-7} to 1×10^{-5}	9×10^{-8}	Sens. Actuators, B, 2015, 212, 214–219
Fluorescence	GQDs	1×10^{-6} to 5×10^{-4}	5×10^{-7}	Microchim. Acta, 2015,182,1723–1731
Fluorescence	GQD-DFOB-Fe^{3+}	1×10^{-7} to 2.6×10^{-5}	2.8×10^{-9}	This assay

Table S2 Glutathione detection: our method *vs.* others.

Method	Material	Linear range (M)	Limit of Detection(M)	Reference
Colorimetry	UiO-66(NH_2) nanoparticles	5×10^{-6} to 1.2×10^{-4}	3.1×10^{-7}	Biosens. Bioelectron., 2016, 81, 465–72
Colorimetry	Fe-MIL-88B(NH_2)	1×10^{-6} to 1×10^{-4}	4.5×10^{-7}	Anal. Methods, 2014, 6, 5647–5651
Colorimetry	Ce-MOF	1.3×10^{-7} to 4×10^{-5}	1.3×10^{-7}	Chem. Commun., 2015, 51, 4635–4638.
Colorimetry	Au nanoparitcles	2×10^{-7} to 9×10^{-7}	3.6×10^{-8}	Biosens Bioelectron., 2015, 68, 668–74
Electrochemistry	Thymine-Hg^{2+}/DNA	—	5×10^{-9}	Chem. Commun., 2014, 50, 8385–8387
Electrochemistry	ZnO/CNTs	6×10^{-9} to 1.6×10^{-4}	2×10^{-9}	Mater. Sci. Eng. C, 2015, 47, 77–84
Electrochemistry	Au-Pd/reduced graphene oxide	1×10^{-6} to 1.2×10^{-5}	1.4×10^{-7}	Analyst, 2016, 141, 2904–2910
Electrochemistry	thymine-Hg^{2+}	1×10^{-9} to 5×10^{-7}	—	Biosens. Bioelectron., 2016, 77, 914–20
Capillary Electrophoresis	Iodoacetic acid/ dansyl chloride	1×10^{-6} to 2×10^{-4}	1×10^{-6}	J. Pharm. Biomed. Anal., 1997, 15, 1435–1441
Surface-enhanced Raman	Mercaptophenol/ gold flowers	2.5×10^{-5} to 9×10^{-4}	2×10^{-7}	Anal. Chem., DOI: 10.1021/acs.analchem. 6b02081
Fluorescence	AuNPs@carbon dots	0 to 1×10^{-7}	6×10^{-9}	ACS Appl. Mater. Interfaces, DOI: 10.1021/acsami.6b06353
Fluorescence	NIR probe (CyR)	5×10^{-7} to 2.5×10^{-5}	1.5×10^{-7}	Anal. Chem., DOI: 10.1021/acs.analchem. 6b02646
Fluorescence	Rhodamine B-based probes	—	1.9×10^{-7}	Sens. Actuators, B, 2016, 237, 431–442
Fluorescence	GQDs-MnO_2	1×10^{-6} to 1×10^{-3}	4.5×10^{-7}	Anal. Methods, 2016, 8, 2366–2374
Fluorescence	carbon quantum dots	4×10^{-8} to 1.3×10^{-5}	4×10^{-8}	Biosens. Bioelectron., 2016, 86, 748–755
Fluorescence	oxTMB and TMPyP	1×10^{-7} to 2×10^{-5}	3×10^{-8}	Biosens Bioelectron., 2016, 81, 268–73
Fluorescence	GQD-DFOB-Fe^{3+}	8×10^{-8} to 2×10^{-5}	3.3×10^{-9}	This assay

Table S3 NADH detection: our method *vs.* others.

Method	Material	Linear range (M)	Limit of Detection(M)	Reference
Colorimetry	Au nanoparticles	0 to 1×10^{-4}	1.25×10^{-5}	ACS Appl. Mater. Interfaces, 2015, 7, 15023–15030
Colorimetry	Au nanoparticles	8×10^{-9} to 8×10^{-6}	8×10^{-9}	Biosens. Bioelectron., 2012, 35, 443–446
Colorimetry	CuNPs@carbon matrix	1×10^{-5} to 1×10^{-3}	5×10^{-8}	Methods Mol. Biol., 2014, 1149, 311–323
Electrochemistry	FeN NPs/N-doped graphene	4×10^{-7} to 7.2×10^{-4}	2.5×10^{-8}	Biosens Bioelectron., 2016, 83, 68–76
Electrochemistry	ZnO/CNTs	1×10^{-6} to 6.5×10^{-4}	3×10^{-5}	Mater. Sci. Eng. C, 2015, 47, 77–84
Electrochemistry	SWCNT-polytyrosine	1.5×10^{-7} to 8.3×10^{-5}	7.9×10^{-9}	Biosens Bioelectron., 2016, 86, 308–14
Electrochemistry	Graphene/pyrrolo-quinoline quinone	3.2×10^{-7} to 2.2×10^{-4}	1.6×10^{-7}	Biosens. Bioelectron., 2016, doi:10.1016/ j.bios.2016.04.092
Electrochemistry	polyethylenimine /graphene oxide	5×10^{-8} to 5×10^{-4}	2×10^{-8}	Biosens. Bioelectron., 2016, doi: 10.1016/ j.bios.2016.05.045
Electrochemistry	poly(o-anisidine) /graphene	1.6×10^{-7} to 1.7×10^{-6}	1.3×10^{-6}	Mater. Sci. Eng. C 2015, 55, 579–91
Capillary Electrophoresis	Mercaptophenol/ gold flowers	2.5×10^{-5} to 9×10^{-4}	2×10^{-7}	Anal. Chem., 2009, 81, 1280–1284
Fluorescence	organic Probes (BA-Resa)	0 to 1×10^{-6}	8.7×10^{-8}	J. Am. Chem. Soc. 2016, 138, 10394−10397
Fluorescence	Cu nanoparticls	5×10^{-7} to 2.5×10^{-5}	1.5×10^{-7}	Talanta, 2016,1, 154:574–80
Fluorescence	Ag nanoparticles	1×10^{-4} to 4×10^{-3}	1×10^{-4}	Anal. Biochem., 2016, 494, 46–48
Fluorescence	CdSe/ZnS	1×10^{-6} to 2.5×10^{-4}	1×10^{-6}	Angew. Chem., Int. Ed., 2009, 48, 309–313
Fluorescence	Ag clusters	1×10^{-5} to 3×10^{-4}	5×10^{-6}	Anal. Chim. Acta., 2015, 886, 151–156
Fluorescence	GQD-DFOB-Fe^{3+}	7×10^{-8} to 1.8×10^{-5}	5.6×10^{-9}	This assay

Table S4 Response time of H_2O_2 detection: our method *vs.* others.

Method	Probe	Response time (Min)	Reference
Colorimetry	Ag NPs/GQDs	5	Anal. Chem. 2014, 86, 6689−6694
Colorimetry	Copper nanoclusters	15	Anal. Chim. Acta., 2013, 762, 83–86
Colorimetry	Magnetic Fe_3S_4 nanoparticles	10	Microchim. Acta, 2016, 183, 625–631
Colorimetry	CuNPs@carbon matrix	20	Chem. Eur. J. 2014, 20, 16377–16383
Colorimetry	V_2O_5 nanorods	5	Sensors, 2016, 16, 584–595
Colorimetry	WC nanorods	20	Biosens.Bioelectron. 2014, 54, 521–527
Colorimetry	Graphene oxide	10	Adv. Mater. 2010, 22, 2206–2210
Colorimetry	Graphene dots	10	Biosens.Bioelectron. 2013, 49, 519–524
Colorimetry	nitrogen-doped GQDs	15	Anal. Chim. Acta., 2015, 869, 89–95
Electrochemistry	gold/Polypyrrole /MWCNTs	4	Sensors, 2013, 13, 3878–3888
Electrochemistry	Copper/Polypyrrole	5	Sensors, 2008, 8, 5141–5152
Fluorescence	Carbon nanodots	10	Anal. Methods, 2014, 6, 1922–1927
Fluorescence	boronate ester-merocyanine-GQDs	25	Anal. Chem., 2016, 88, 4833–4840
Fluorescence	AgNP-DNA@GQDs	35	Anal. Chem., 2014, 86, 12348–12354
Fluorescence	GQD-DFOB-Fe^{2+}	3	This assay

Table S5 H_2O_2 detection: our method *vs.* others.

Method	Material	Linear range (M)	Limit of Detection(M)	Reference
Colorimetry	Nitrogen-doped GQDs	2×10^{-5} to 1.2×10^{-3}	5.3×10^{-6}	Anal. Chim. Acta., 2015, 869, 89–95
Colorimetry	Au clusters	1×10^{-7} to 2×10^{-5}	2×10^{-8}	Biosens.Bioelectron. 2011, 26, 3614–3619
Colorimetry	AgNPs@GQDs	1×10^{-7} to 1×10^{-4}	3.3×10^{-7}	Anal.Chem.2014, 86, 6689–6694
Colorimetry	GQDs	1×10^{-4} to 1×10^{-2}	2×10^{-5}	J. Mater. Chem., 2013, 1, 4676–4684
Colorimetry	Graphene oxide	5×10^{-8} to 1×10^{-6}	5×10^{-8}	Adv. Mater. 2010, 22, 2206–2210
Colorimetry	V_2O_5 nanorods	1×10^{-6} to 5×10^{-4}	1×10^{-6}	Sensors 2016, 16, 584–595
Colorimetry	Polyoxometalate	1×10^{-6} to 2×10^{-5}	4×10^{-7}	ChemPlusChem, 2012, 77, 541–544
Colorimetry	Carbon nitride dots	1×10^{-6} to 1×10^{-4}	4×10^{-7}	RSC Adv., 2012, 2, 411–413
Colorimetry	Carbon nanodots	1×10^{-6} to 1×10^{-4}	2×10^{-7}	Chem. Commun., 2011, 47,6695–6697.
Colorimetry	Pt–DNA complexes	9.8×10^{-4} to 2×10^{-2}	3.3×10^{-4}	Anal. Methods, 2012, 4,2183–2187
Colorimetry	Hemin-graphene hybrid nanosheets	5×10^{-8} to 5×10^{-4}	2×10^{-8}	Sens. Actuators, B, 2011, 160,295–300
Electrochemistry	GQDs	2×10^{-6} to 8×10^{-3}	7×10^{-8}	Nanoscale, 2013, 5, 1816–1819
Electrochemistry	GQDs	1×10^{-3} to 1×10^{-2}	2×10^{-5}	Carbon, 2015, 81, 514–524
Electrochemistry	Urchin-like Co_3O_4	1×10^{-7} to 5×10^{-5}	1×10^{-7}	J. Solid State Chem., 2015, 228, 226–231.
Electrochemistry	Carbon quantum dots/octahedralCu_2O	5×10^{-6} to 5×10^{-3}	2.8×10^{-6}	Sens. Actuator B, 2015, 206, 735–743
Electrochemistry	Nanoporous magnesium oxide	5×10^{-5} to 5×10^{-2}	3.3×10^{-6}	RSC Adv., 2015, 5, 86485–86489
Electrochemistry	CdS nanoparticles	1×10^{-6} to 1.9×10^{-3}	2.8×10^{-6}	J. Mol. Catal. A: Chem., 2012, 358, 1–9

Electrochemistry	FeSe NPs	5×10^{-6} to 1×10^{-4}	3×10^{-6}	ACS Appl. Mater. Interfaces, 2012, 4, 1919–1927.
Electrochemistry	Iron oxide NPs/CNT	9.9×10^{-5} to 6×10^{-3}	5.4×10^{-5}	Sens. Actuators, B, 2009, 138, 182–188.
Electrochemistry	Fe_2O_3 nanoparticles	2×10^{-5} to 3×10^{-4}	7×10^{-6}	J. Mol. Catal. A: Chem., 2012, 360, 71–77
Photoelectrochemistry	gold nanoclusters	0 to 4×10^{-3}	3.5×10^{-5}	Biosens.Bioelectron., 2015, 67, 296–302
Electrophoresis	dichlorofluorescein	5×10^{-7} to 5×10^{-5}	2×10^{-7}	Electrophoresis 2009, 30, 1983–1990
Chemluminescence	$CoFe_2O_4$ NPs	1×10^{-7} to 4×10^{-6}	2×10^{-8}	Talanta, 2010, 82, 377–383
Fluorescence	Carbon nanodots	2.5×10^{-8} to 5×10^{-5}	1×10^{-8}	Anal. Methods, 2014,6, 1922–1927
Fluorescence	Au nanoclusters	1×10^{-6} to 1×10^{-4}	8×10^{-7}	Anal. Chem. 2015, 87, 10362–10367.
Fluorescence	Carbon dots	2×10^{-5} to 2×10^{-2}	5×10^{-6}	Talanta, 2015, 144, 1308–1315
Fluorescence	Cu nanoclusters	5×10^{-7} to 1×10^{-5}	4×10^{-7}	Spectrochim. Acta. A,2014,118,315–320
Fluorescence	AgNP-DNA@GQDs	4×10^{-7} to 2×10^{-4}	1×10^{-7}	Anal. Chem. 2014, 86, 12348–12354
Fluorescence	boronate ester-merocyanine-GQDs	2×10^{-7} to 4×10^{-5}	5×10^{-8}	Anal. Chem., 2016, 88, 4833–4840
Fluorescence	FeTMPyP@GQDs	2×10^{-6} to 3×10^{-4}	3×10^{-7}	Chem. Eur. J., 2015, 21, 9343–9348
Fluorescence	GQD-DFOB-Fe^{2+}	3×10^{-8} to 3.2×10^{-5}	1.4×10^{-9}	This assay

Table S6 ClO^- detection: our method *vs.* others.

Method	Material	Linear range (M)	Limit of Detection(M)	Reference
Colorimetry	Au nanoparticles	0 to 5.3×10^{-5}	2×10^{-6}	Sensor. Actuat. B, 2012, 161, 229–234
Colorimetry	*p*-methoxyphenol derivative	0 to 1×10^{-4}	8×10^{-7}	Org. Biomol. Chem., 2011, 9, 5560–5563
Colorimetry	Au nanoparticles	0 to 5×10^{-6}	1.5×10^{-6}	Analyst, 2012, 137, 2806–2812
Electrochemistry	Pt indicator electrode	3.7×10^{-6} to 6×10^{-5}	2×10^{-7}	Electroanalysis, 2005, 17, 769–775
Electrochemistry	Poly MnTAPP/ nano Au	2.4×10^{-5} to 1×10^{-2}	2.4×10^{-5}	J. Electroanal. Chem., 2011, 661, 322–328
Electrochemistry	Ferrocene compounds	1×10^{-6} to 2×10^{-4}	5×10^{-7}	Int. J. Electrochem. Sci. 2015, 10, 3260–3268
Electrochemistry	silver amalgam film electrode	6×10^{-7} to 7×10^{-6}	1.8×10^{-7}	Talanta, 2013, 117, 242–249
Fluorescence	tetraphenylethene	0 to 1×10^{-5}	4.7×10^{-7}	Chem. Commun., 2016, 52, 7288–7291
Fluorescence	7-nitrobenzox adiazole	0 to 1×10^{-5}	5.2×10^{-8}	Talanta, 2016, 147, 468–72
Fluorescence	Europium-single walled carbon nanotube	1×10^{-7} to 4×10^{-6}	9×10^{-8}	Analyst, 2012, 137, 1872–1875
Fluorescence	Carbon dots	1×10^{-7} to 1×10^{-5}	5×10^{-8}	Analyst, 2013, 138, 6551–6557
Fluorescence	Metal-Organic Frameworks Nanoplates	5×10^{-8} to 1.5×10^{-5}	4×10^{-4}	Anal. Chem., 2016, 88, 3413–3420
Fluorescence	Coumarin-Based Probe	0 to 5×10^{-8}	2×10^{-8}	J. Fluoresc., 2016, 26, 403–406
Fluorescence	7-Hydroxycoumarin	0 to 2.4×10^{-4}	5.68×10^{-8}	Spectrochim. Acta A, 2016, 166, 79–83
Fluorescence	GQD-DFOB-Fe^{2+}	2.5×10^{-8} to 2.5×10^{-5}	2.1×10^{-9}	This assay

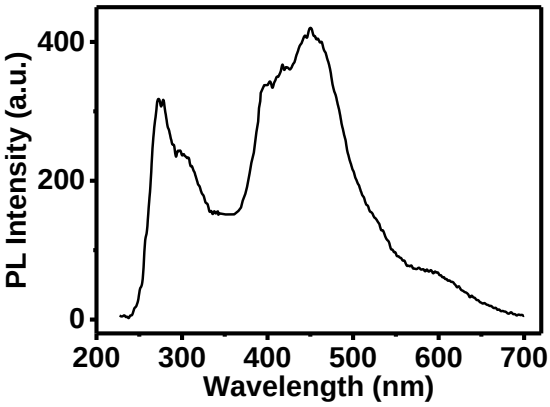

Figure S1. Excitation spectra of 0.1 mg/mL graphene quantum dots in PBS buffer solution (pH 7.0) with emission at 527 nm.

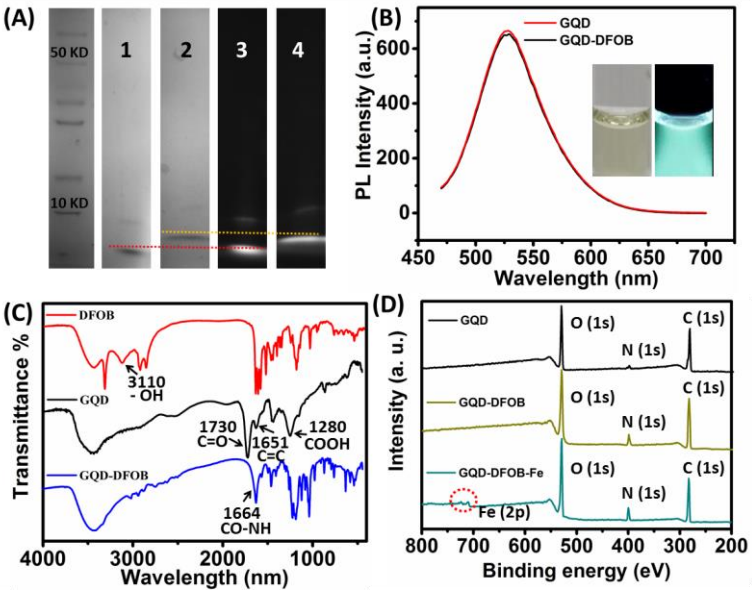

Figure S2. (A) Electrophoresis gel images of graphene quantum dots (GQDs) (1 and 3) and graphene quantum dots-desferrioxamine B (GQD-DFOB) samples (2 and 4). Lanes 1 and 2 were imaged under white light, while the fluorescence images for lanes 3 and 4 were taken under illumination by a xenon lamp (488 nm filter for excitation; 505 nm filter for emission). (B) Photoluminescence (PL) spectra of GQD and GQD-DFOB suspensions at the excitation wavelength of 450 nm. Inset shows photographs of GQD-DFOB suspension under daylight (left) and 365 nm UV (right). (C) Fourier transform infrared spectroscopy characterization of DFOB, GQD and GQD-DFOB. (D) X-ray photoelectron spectroscopy characterization of GQD, GQD-DFOB, and GQD-DFOB-Fe^{3+}.

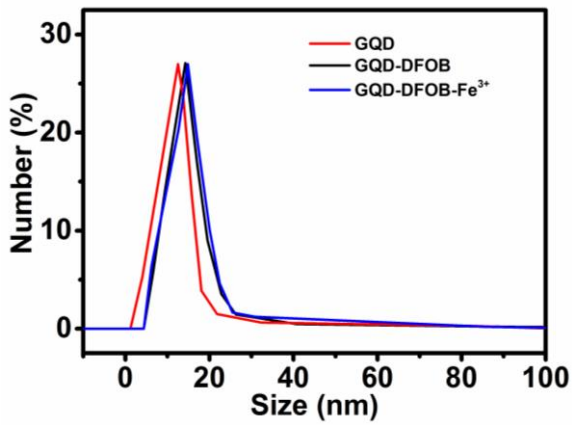

Figure S3. Dynamic light scattering measurements of 0.1 mg/mL bare GQD, GQD-DFOB and GQD-DFOB-Fe^{3+}, respectively.

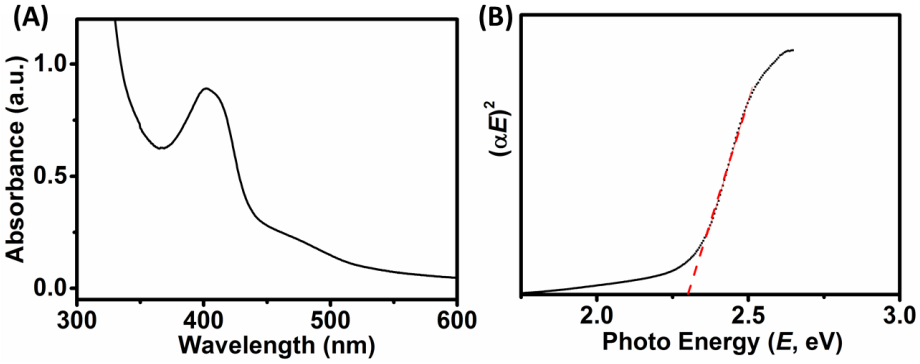

Figure S4. (A) Optical absorption spectrum of GQDs (0.1 mg/mL) in PBS (pH 7.0). (B) Plots of $(\alpha E)^2$ against photon energy (E) for the GQDs solution, where α is the absorbance. The dashed line is the linear fitting.

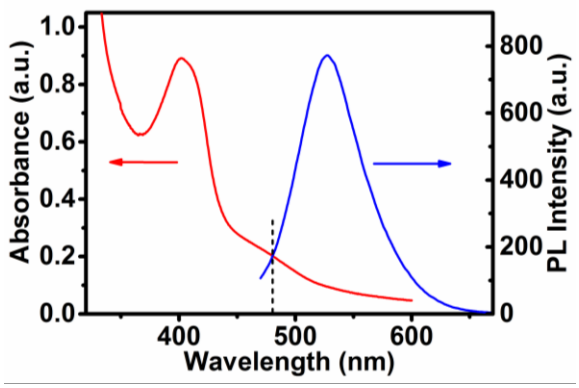

Figure S5. The intersection point (at 488 nm) between absorption and emission spectra of GQDs in PBS (pH 7.0).

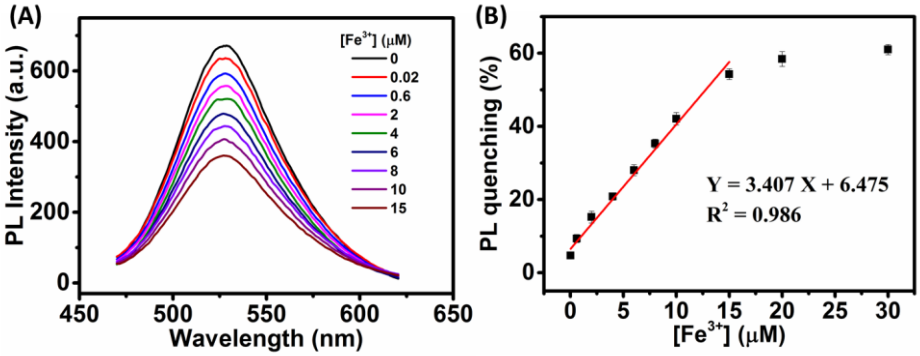

Figure S6. (A) Photoluminescent spectra of 0.1 mg/mL GQD-DFOB in PBS (pH 7.0) chelated with different concentrations of Fe^{3+}. (B) Photoluminescent quenching efficiency *vs.* Fe^{3+} concentration. The error bars indicate the standard deviation from 3 measurements.

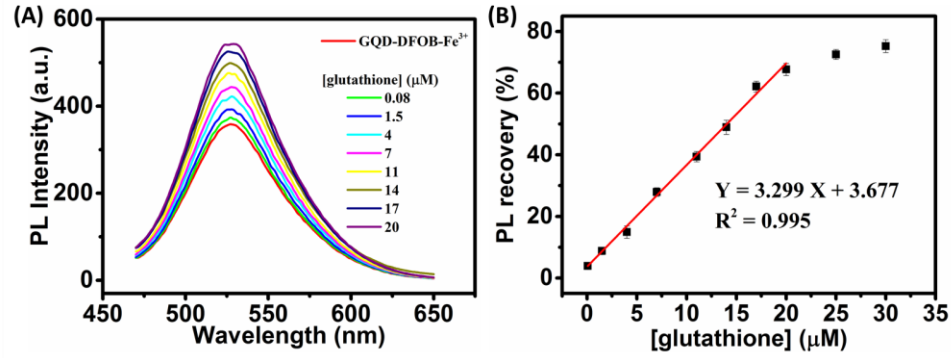

Figure S7. (A) Photoluminescence spectra of 0.1 mg/mL GQD-DFOB-Fe^{3+} in PBS (pH 7.0) containing different concentrations of glutathione. (B) Photoluminescence quenching efficiency *vs.* glutathione concentration. The error bars indicate the standard deviation from 3 measurements.

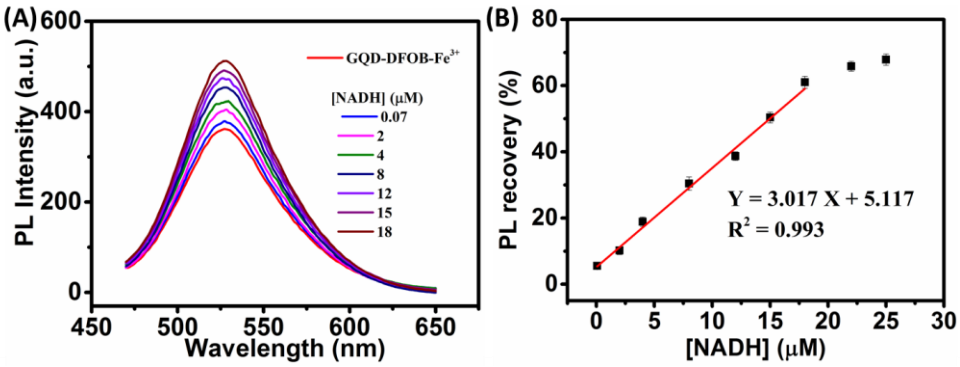

Figure S8. (A) Photoluminescence spectra of 0.1 mg/mL GQD-DFOB-Fe^{3+} in PBS (pH 7.0) containing different concentrations of NADH. (B) Photoluminescence quenching efficiency *vs.* NADH concentration. The error bars indicate the standard deviation from 3 measurements.

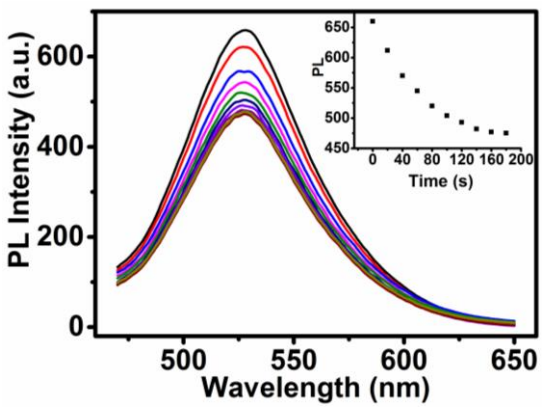

Figure S9. Time-dependent (0–3 min) photoluminescence quenching of 0.1 mg/mL GQD-DFOB-Fe^{2+} in PBS (pH 7.0) containing 10 μM H_2O_2. Inset shows how fluorescence intensity of GQD-DFOB-Fe^{2+} evolves with time in the presence and absence of H_2O_2.

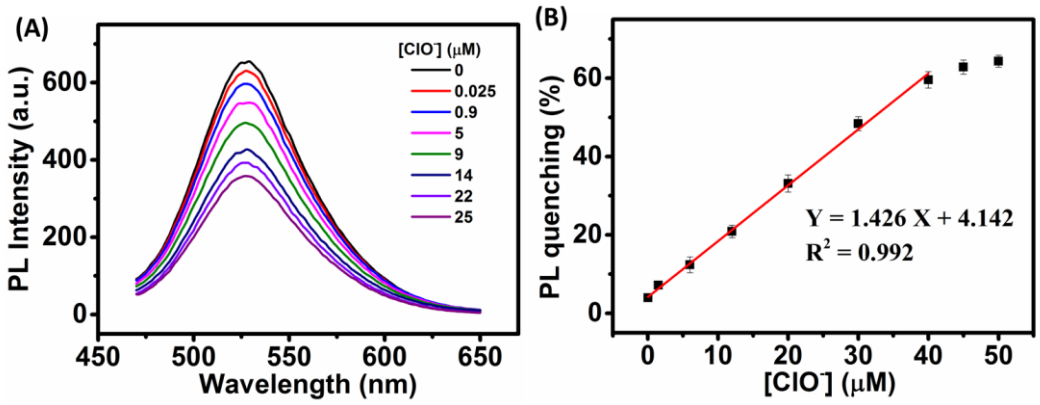

Figure S10. (A) Photoluminescence spectra of 0.1 mg/mL GQD-DFOB-Fe^{2+} in PBS (pH 7.0) containing different concentrations of ClO^-. (C) Photoluminescence quenching efficiency *vs.* ClO^- concentration. The error bars indicate the standard deviation from 3 measurements.

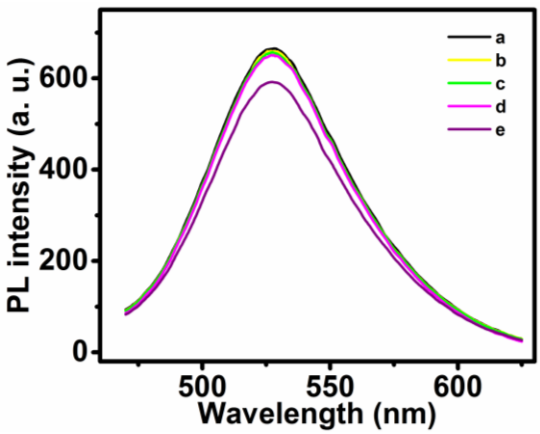

Figure S11. Photoluminescence spectra of GQD-DFOB-Fe^{2+} suspension: (a) freshly prepared sample; (b) left in ambient for 1h at room temperature; (c) left in ambient for 2h at room temperature; (d) in deareated buffer (by purging with nitrogen for 15min) for 7 days at 4 ^{0}C; (e) in ambient for 7 days at 4 ^{0}C. Excitation wavelength at 450 nm.

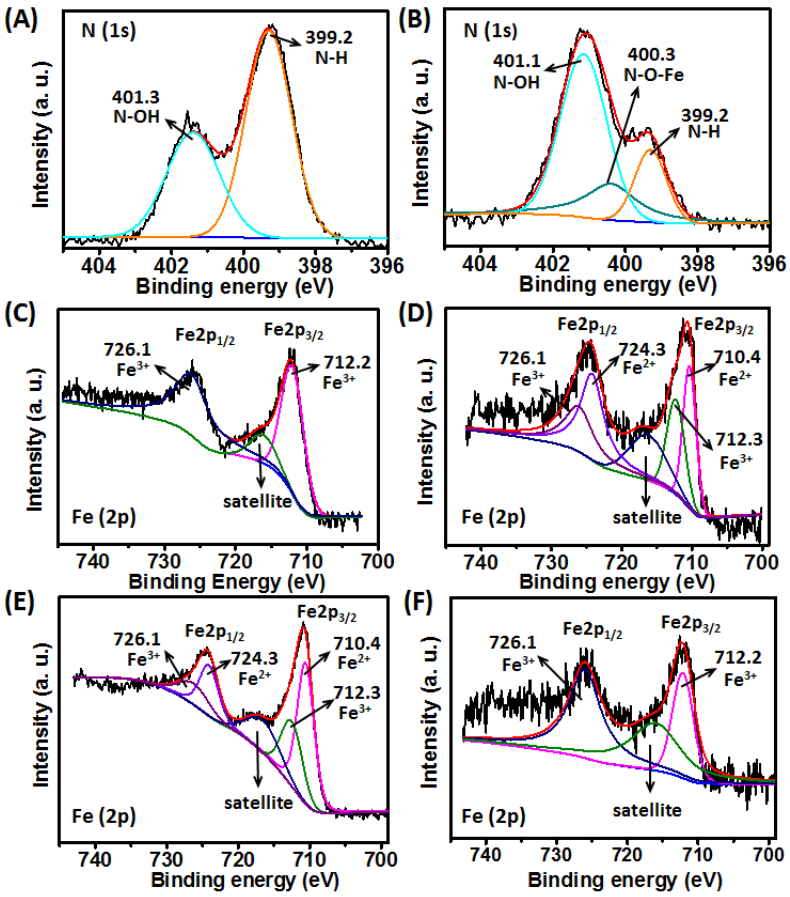

Figure S12. The XPS N1s spectra of GQD-DFOB without/with chelated Fe^{3+} (A, B); Fe2p spectra of GQD-DFOB-Fe^{3+} before and after addition of 100 μM AA (C, D); and Fe2p spectra of GQD-DFOB-Fe^{2+} before and after addition of 10 μM H_2O_2 (E, F).

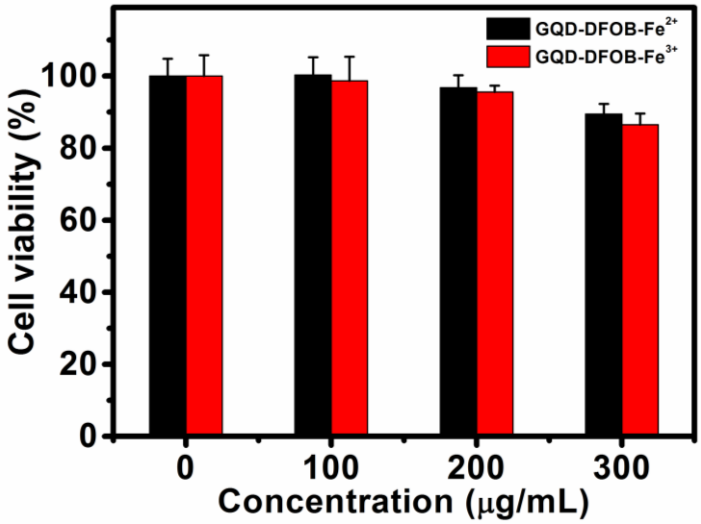

Figure S13. MTT cytotoxicity analysis of Hela cells incubated with GQD-DFOB-Fe^{2+} or GQD-DFOB-Fe^{3+} for 24 h (means ± standard deviation, n=4).

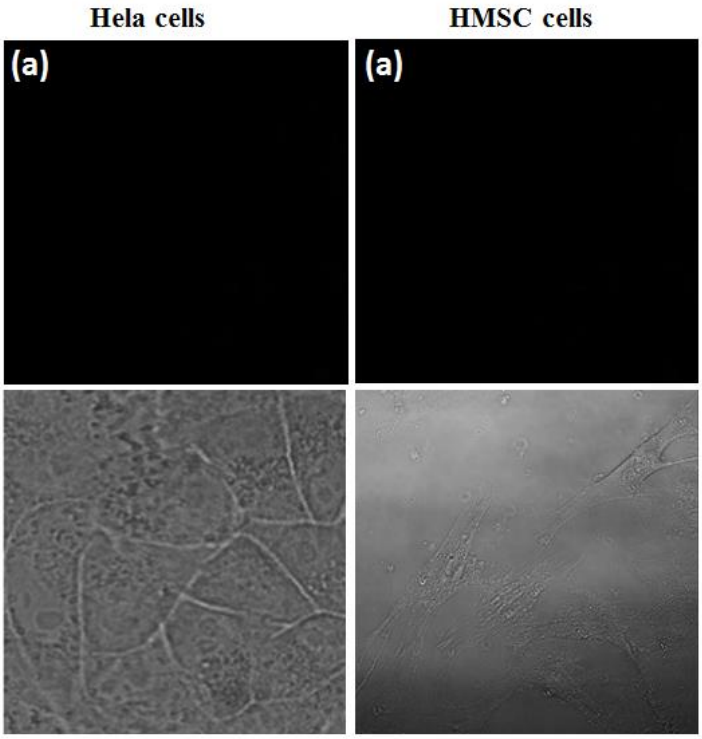

Figure S14. Confocal (top) and bright-field (bottom) images of Hela cells (left) or human mesenchymal stem cells (right) without incubation of GQD probes.

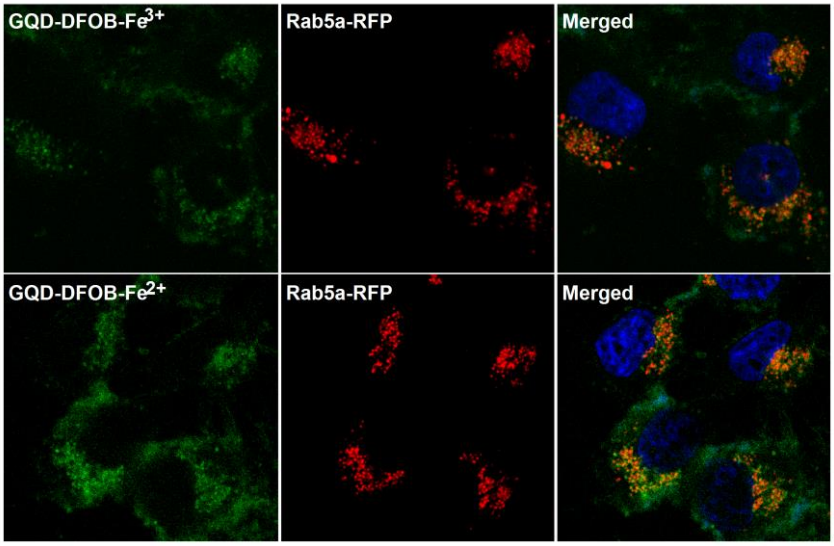

Figure S15. Confocal images of Hela cells overexpressed with Rab5a-RFP conjugate (Rab5a is an endosomal marker; FRP is a red fluorescence protein; from CellLight®Early Endosomes-RFP, BacMam 2.0), and pre-incubated (1 h) with 0.1 mg/mL GQD-DFOB-Fe^{3+} (top) and GQD-DFOB-Fe^{2+} (bottom). Excitation and emission wavelengths for Rab5a-RFP are 555 and 584 nm respectively.

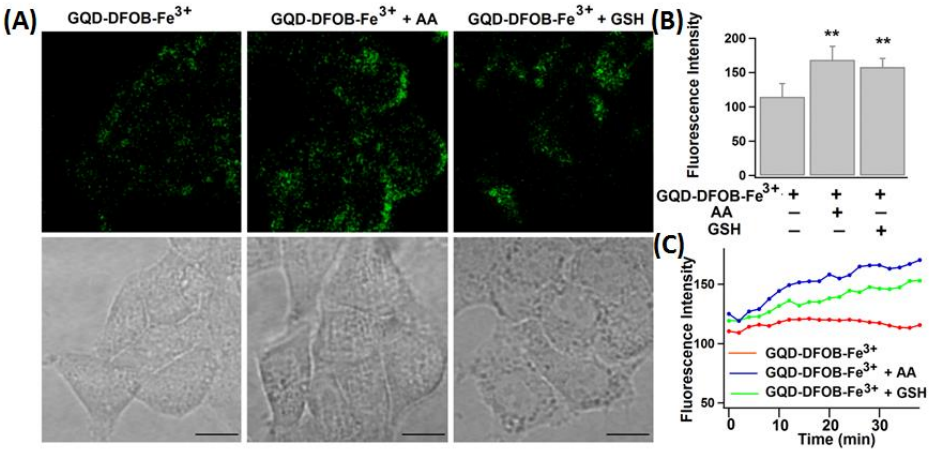

Figure S16. Live cell imaging of intracellular reductive stress using GQD-DFOB-Fe^{3+}. (A) Confocal (top) and bright-field (bottom) images of Hela cells pre-incubated for 1 h with 0.1 mg/mL GQD-DFOB-Fe^{3+}, without or with subsequent addition of 100 µM ascorbic acid (AA) or glutathione (GSH). Scale bar = 10 µm. (B) Statistics (mean ± SD) of the fluorescence intensity of GQD-DFOB-Fe^{3+} loaded Hela cells (n=12 – 15) in the absence or presence of AA or GSH. Student's t test, ** $p < 0.01$ vs. without treatment. (C) The change of averaged fluorescence intensity of 12 GQD-DFOB-Fe^{3+} loaded cells without or with stimulation of AA or GSH (2 min interval).